

Towards a compact cold atom frequency standard based on coherent population trapping

Francois-Xavier Esnault, Elizabeth Donley and John Kitching

Atomic Devices and Instrumentation group

Time and frequency Division, National Institute of Standards and Technology

325 Broadway, Boulder CO 80305, USA

Email: edonley@nist.gov

Abstract—We describe the main features of a cold atom frequency standard based on coherent population trapping (CPT). We explain our particular CPT configuration and our experimental setup, and present simulations of the expected performance (stability and major systematics).

I. INTRODUCTION

A. Background on miniaturized clocks

The performance of atomic clocks based on Coherent Population Trapping (CPT) has improved considerably over the last few years in terms of stability and reliability [1], [2], [3]. Frequency stabilities in the low $10^{-10} \tau^{-1/2}$ range are now realized within package volumes a few tens of cubic centimeters [3]. Nevertheless, a significant frequency drift ($\geq 10^{-12}/\text{day}$) is observed on these devices. The use of wall coatings and buffer gases, which are required for high-contrast narrow-linewidth CPT resonances, tends to degrade the long-term stability through cell aging and large temperature-dependent pressure shifts. Light shifts also play a role in the drift of CPT-based clocks, which we will ultimately study experimentally with the apparatus that we describe in this work.

B. Project goals

To circumvent these issues, we recently started a study of a microwave CPT frequency standard based on laser-cooled atoms (CA-CPT). Cold atoms can provide the required accuracy, while the all-optical CPT interrogation enables good stability through narrow atomic resonances [1] and allows miniaturization of the physics package by eliminating the microwave cavity. This project aims at reaching a frequency stability of better than $10^{-11} \tau^{-1/2}$ and an accuracy around 10^{-13} within a miniaturized physics package. Our work focuses both on the experimental realization and the metrological evaluation of a CA-CPT clock and on efficient ways of producing a cold atom sample in a millimetric volume. To our knowledge there is no published result on a CA-CPT frequency standard.

C. Cold-atom vs vapor-cell clock

Here we would like to emphasize the fundamental differences between CPT clocks based on cold atoms and clocks based on vapor cells filled with buffer gases. The main differences for the cold-atom CPT clock are:

- Excited state hyperfine structure is resolved

- Cyclic operation
- No buffer gases (no collisional shifts, no decoherence)
- Long interrogation period
- No collisional homogeneous broadening of optical transitions
- Saturation intensity is much smaller (less power needed to interrogate)
- Small atom number in the sample (smaller signal-to-noise ratio (SNR))
- Sensitivity to gravity/residual accelerations (Doppler effect)

II. CPT INTERROGATION

Many schemes and configurations with differing atom type, optical excitation line, light polarization, etc. have been proposed to improve the metrological properties of a clock based on a CPT resonance [1]. We want to maximize the signal to noise ratio (SNR), which is usually set by the overall atomic density of the sample, and the contrast C of the CPT peak, which is determined by the proportion of atoms involved in the clock transition. This can be achieved, for example, with a polarization configuration that does not involve so-called “trap states” (extreme m_F sublevels) [4], and by using a larger intensity in the CPT beams to increase the pumping rate into the “dark state”. This latter option has two major drawbacks. A large intensity broadens the resonance, so that the high contrast is quickly counter-balanced by a broader linewidth $\Delta\nu$; secondly, it increases the magnitude of the second-order Stark shift (light shift).

The sequence and configuration that we propose, a pulsed Ramsey-like sequence on a cold ^{87}Rb sample by use of a $\text{lin}||\text{lin}$ configuration [5], can achieve high contrast without being limited by power broadening and large light shifts. The advantages of this approach are described in the following subsections.

A. lin parallel lin configuration

The $\text{lin}||\text{lin}$ configuration was first proposed and studied by Taichenachev *et al.* in [5] and then investigated further in [6], [7], [8], [9], [10]. This scheme is most efficient when the coupling occurs between ground states of total angular momenta $F = 1, 2$ and an excited state of total angular momentum $F' = 1$. Moreover, good spectral resolution of

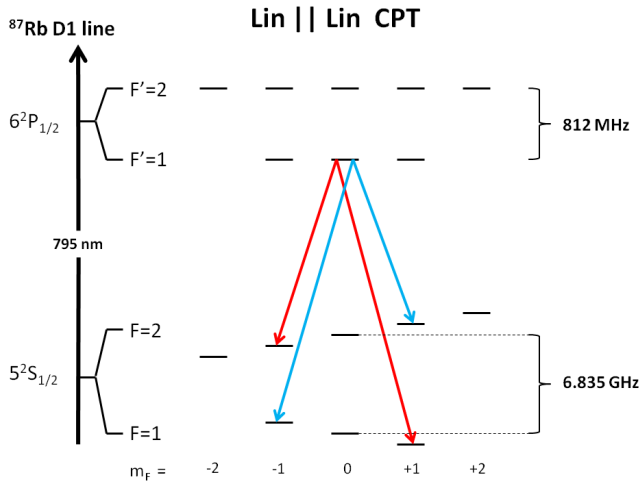


Fig. 1. Energy diagram of the ^{87}Rb D1 line at 795 nm and transitions involved in the $\text{lin}||\text{lin}$ configuration.

the excited hyperfine levels is required. These conditions can be met fully for the D1-line of ^{87}Rb and partially for the D2-line with laser cooled atoms. The CPT resonance is the superposition of two Λ systems (see Fig. 1) connecting the ground state sublevels $|F = 1, m_F = \pm 1\rangle$ and $|F = 2, m_F = \mp 1\rangle$ through the excited level $|F' = 1, m_F = 0\rangle$. Thus, four out of eight sublevels, or about half of the atoms, are involved in the clock transition. Indeed, contrasts of up to 40 % have been reported in [5] and of 25 % in [8]. From an experimental perspective, this scheme is well suited for a frequency modulated diode laser, as both beams have the same polarization. Magnetic sensitivity properties are discussed in section IV-C.1

B. Pulsed interrogation

The idea of using Ramsey-like pulsed interrogation with CPT interactions was pioneered by Hemmer and Ezekiel at MIT during the late 80s, who used a thermal sodium beam and spatially separated interactions [11], [12], [13]. More recently, several groups [14], [15] have used that technique in alkali vapor cells with two optical pulses separated in time by T_R . The first pulse (duration $\tau_p \approx 20 \mu\text{s}$) pumps the atoms into the “dark state”; then the atoms evolve freely for a period of T_R after which the second pulse (duration τ_m) measures the accumulated phase. An absorption measurement gives rise to an interference pattern typical of Ramsey interrogation. The detection pulse duration has to be as small as possible [14]; we conservatively set it to 5 μs .

In this scheme, because the atoms primarily evolve most of the time without interacting with the light fields, the linewidth $\Delta\nu$ no longer depends on the atomic saturation but is Fourier limited and scales as $1/(2T_R)$. For a miniaturized cold atom clock, the interrogation time is limited by the size of the cell and acceleration due to gravity to about 10 ms in a 1 mm cell leading to a 50 Hz linewidth. As power broadening is

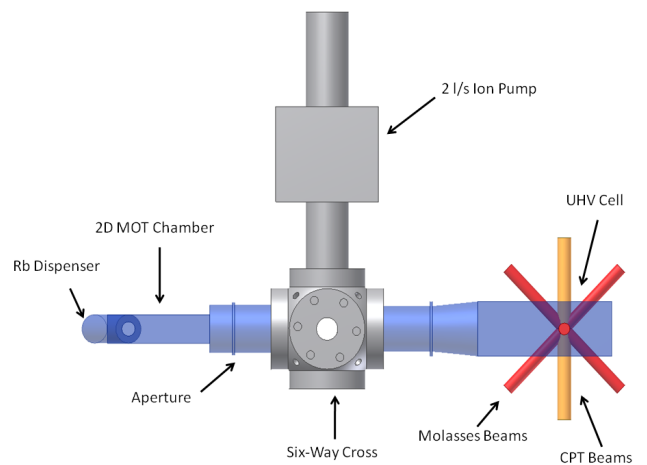


Fig. 2. Vacuum chamber.

no longer an issue, we can increase the laser intensity to get higher pumping rates and improved resonance contrast. Moreover, this technique greatly reduces the light shift (see section IV-C.2).

III. EXPERIMENTAL SET UP

We are currently building our experimental setup. This section presents some of our designs and ideas concerning the vacuum chamber, the cooling system geometry, and the optical phase lock loop required to generate the CPT beams.

A. Vacuum chamber

We use a vacuum chamber produced by *Cold Quanta, Inc.*¹ for atom-chip BEC experiments. The chamber is shown in Fig. 2 and described in detail in [16], [17]. The main chamber, where a 3D optical molasses will be realized, is separated from a 2D-MOT zone containing a Rb dispenser by two pinholes of 1 mm diameter, ensuring differential pumping. The vacuum level in the main chamber is currently below 10^{-7} Pa thanks to a 2 L/s ion pump and another getter pump.

We will mount the whole chamber horizontally to realize CPT interrogation parallel or perpendicular to gravity. Two Helmholtz coils will be used to define a proper quantization axis along the CPT beams.

B. laser cooling setup

The 2D-MOT zone will be created by two elliptical retroreflected beams in a chamber with a clear aperture of $12 \times 12 \times 25 \text{ mm}^3$ and the quadrupole field will be generated by permanent magnets. A pushing beam will allow a 2D⁺-MOT geometry. The flux of cold atoms will load a standard $\text{lin} \perp \text{lin}$ 3D optical molasses.

¹Products or companies named here are cited only in the interest of complete scientific description, and neither constitute nor imply endorsement by NIST or by the US government. Other products may be found to serve equally as well.

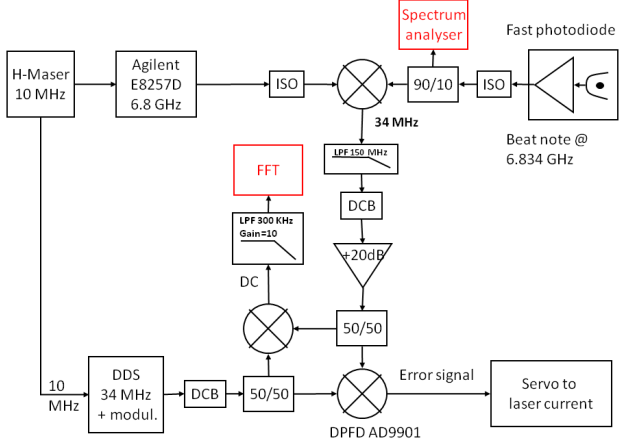


Fig. 3. Optical phase lock loop design

To save laser power we plan to use a “recycling” geometry developed at JPL [18]. In this scheme the six molasses beams are produced by two incoming and counter-propagating beams with each one recycled twice to perform 3D cooling. This method ensures that the laser intensity is balanced for each of the three pairs of beams, regardless of the optical losses experienced on the beam paths (atomic absorption, optics transmission) even if it is not balanced between different pairs.

C. Optical PLL setup

In many cases, the bichromatic laser field needed for excitation of the CPT resonances is generated by modulating the injection current of a diode laser. This produces a comb of optical frequencies of varying amplitudes. The unwanted residual sidebands in this comb degrade the clock performance by contributing to detection noise and the AC Stark shift, but they do not contribute to the CPT signal.

To avoid spurious sidebands in the CPT light we have chosen to use two independent phase-locked lasers. We will use two DFB/DBR lasers with a typical 1 MHz linewidth rather than extended cavity lasers. The optical beat note is realized around the ^{87}Rb hyperfine splitting at 6.834 GHz. The design of the optical phase lock loop is shown in Fig. 3. The amplified optical beat note is mixed with a 6.8 GHz signal coming from a microwave synthesizer (referenced to a 10 MHz H-Maser signal), filtered, amplified, and compared with a 34 MHz signal coming from a direct digital synthesizer inside a digital phase frequency detector (DPFD AD9901). This DPFD provides an error signal used to phase lock the two lasers through feedback on the slave laser’s current.

IV. EXPECTED OPERATION AND PERFORMANCE

In this section we derive the expected performance of our clock design with parameter values as realistic as possible.

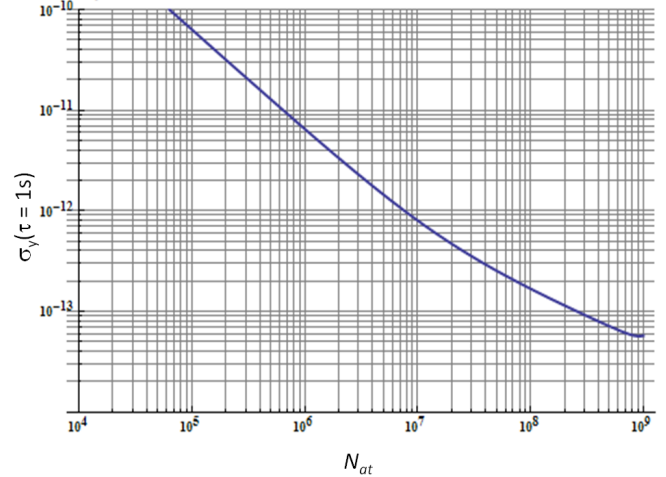


Fig. 4. Estimated short term stability as a function of total atom number in the optical molasses N_{at} . Parameters are: $T_c = 0.1$ s; $\tau_m = 5 \mu\text{s}$; $T_R = 10$ ms; $Sat = 0.01$. Here Sat is the saturation parameter.

A. Experimental parameters

- **Cooling beam size.** For a miniaturized clock package, the cooling beam size must be small. A major goal of this experiment is to see how far the size of a cold atom cloud can be reduced while maintaining performance. We will study the atom number and clock performance for beam diameters in the 1 to 5 mm range.
- **Interrogation period.** Given these size constraints we will limit the interrogation period T_{int} to 10 ms so that the free fall of the cold atom cloud does not exceed 0.5 mm. This ensures that the cloud experiences pulses of nearly equal intensity during the Ramsey interrogation and gives rise to a maximal contrast.
- **2D MOT and 3D optical molasses.** According to [16] and [17], with 120 mW of overall power these systems typically trap up to $N_{max} = 2 \times 10^9$ atoms and have a loading time constant, τ_{load} , of 4 s inside the main chamber. The number of trapped atoms, N_{at} , is thus given by $N_{at} = N_{max}(1 - e^{-T_{cool}/\tau_{load}})$. However, these numbers have to be rescaled for our system, since we plan to use only 30 mW of cooling light and smaller beams. We think that $N_{max} = 10^8$ is a reasonable value.
- **CPT resonance and contrast.** For absorption imaging, we estimate the contrast (defined as CPT peak amplitude over background) to be 0.3 % for $N_{at} = 10^6$ atoms in the cloud and with 50 % of them involved in the CPT interrogation (e.g. pumped into the “dark state”).

B. Noise and Frequency stability

Taking into account electronic noise, optical shot noise, and atomic shot noise, we estimate the short-term frequency stability of the clock as a function of N_{at} . For 10^6 atoms we obtain a short-term stability around 7×10^{-12} (see Fig. 4).

C. Systematics

We expect the main systematic frequency shifts to arise from magnetic-field shifts, light shifts, and Doppler shifts, each of which are discussed below.

1) *Magnetic field*: The CPT resonance used in the *lin||lin* scheme as a frequency reference is the sum of two Λ systems (see Fig. 1). Both transitions have the same quadratic sensitivity to magnetic field; but due to the nuclear spin interaction, these two CPT resonances exhibit a weak linear splitting. The overall magnetic shift for these two transitions is given by $\Delta\nu_{mag} = 430 \text{ Hz}/G^2 \pm 2.8 \text{ kHz}/G$. For small magnetic fields (e.g. for magnetic shifts smaller than the CPT linewidth), this linear splitting leads only to a broadening of the measured resonance, which does not preclude the use of this scheme as a frequency standard. Only for relatively high magnetic fields can the transitions be resolved [19].

However, with our Ramsey-like interrogation and typical magnetic field of tens of milligauss, we must be careful, as this linear magnetic splitting (5.6 Hz/mG) is comparable to the expected linewidth $\Delta\nu$ (about 50 Hz). We have to apply the proper magnetic field such that the interference patterns coming from the two Λ systems add up constructively, as pointed out in [20]. If the magnetic field is too large, then the central Ramsey fringe will be broadened, or even washed out, by the magnetic-field shifts.

2) *Light shifts*: Due to the presence of optical light fields, atomic energy levels experience AC Stark shifts, usually referred to as light shifts. For a two-level system in the presence of a single monochromatic light field, the energy of each state is shifted symmetrically by an amount $\hbar\Delta_{LS}$, where

$$\Delta_{LS} = \frac{1}{4} \frac{|\Omega|^2 \Delta_{opt}}{\Gamma^2/4 + \Delta_{opt}^2}. \quad (1)$$

Ω is the Rabi frequency, Δ_{opt} is the optical detuning, and Γ is the radiative decay rate.

Those shifts have a significant magnitude in most CPT-based operating devices ($\Delta\nu/\nu \approx 10^{-9}$) and are usually proportional to beam intensity. They are a major source of instability and have been extensively investigated for vapor cell clocks [21], [22], [1].

In our case the complete description of a real multi-level system interacting with two resonant light fields is rather complicated, and because of the coherent nature of the CPT phenomenon, we have to distinguish between non-resonant ($|\Delta_{opt}| \gg \Gamma$) and resonant ($|\Delta_{opt}| \approx \Gamma$) couplings.

To evaluate the non-resonant shift, we have to consider all possible couplings induced by the light fields for each state involved in the clock transition (~ 20 couplings). The overall non-resonant frequency shift is the difference between clock states' shifts and consists of a sum of expressions similar to Eq. 1. It can be written as a linear combination of both beam intensities, and fortunately, we can cancel it by choosing the proper intensity ratio because the hyperfine ground states shifts are of the same sign but shift proportional to the intensity with different coefficients. In our case, this “magic” intensity ratio has been computed to be 2.42 for $\Delta_{opt} = 0$. Note that this

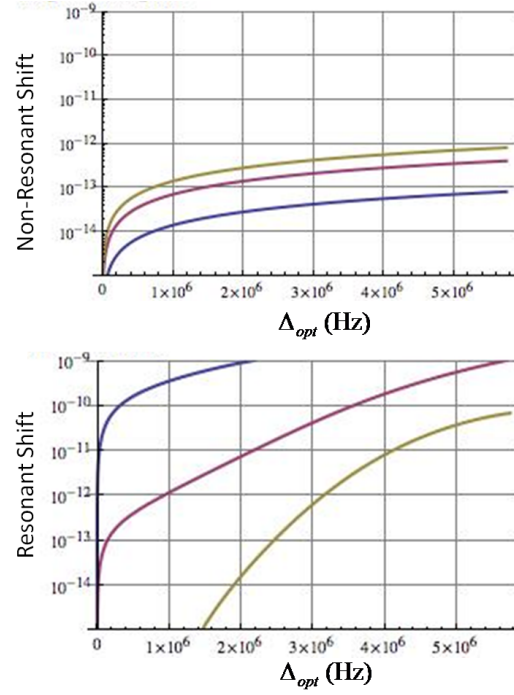


Fig. 5. Relative frequency shifts due to resonant and non resonant light shifts (in absolute value) as a function of optical detuning for different saturation parameters 0.01 (blue), 0.05 (red) and 0.1 (yellow). Laser intensities are set at the magic ratio. All curves are odd functions of optical detuning but are shown only for positive detuning because of log scale. Parameters are : $\tau_p = 20 \mu\text{s}$; $T_R = 10 \text{ ms}$; $\Delta\rho_0 = 1$.

cancellation technique can also be achieved for modulated-laser based clocks by choosing the proper carrier-to-sideband intensity ratio [8]. From an experimental point of view, we computed the sensitivity of the relative frequency shift to optical detuning (around optical resonance) and optical power variations (around the magic ratio) to be

$$\frac{d(shift)}{d(\Delta_{opt})} = 10^{-12} * Sat/\text{MHz} \quad (2)$$

$$\frac{d(shift)}{d(ratio)} = 4.10^{-11} * Sat, \quad (3)$$

where $Sat = I/I_{sat}$ is the total optical saturation, where I_{sat} is the saturation intensity (typ: $Sat = 0.01$). Simulations are shown in Fig. 5.

Resonant AC Stark shifts have been studied in detail both theoretically and experimentally by Hemmer *et al.* in [13] on an atomic beam. Their most striking and counterintuitive result is that the light shift flattens out around optical resonance with increased integrated intensity (e.g., $\Omega^2\tau_p$) (see Fig. 5).

For a small optical detuning ($|\Delta_{opt}| \ll \Gamma$) and equal Rabi

frequencies², the frequency shift can be written as

$$\Delta\nu_{LS} \approx -\frac{\Delta\rho_0\Delta_{opt}}{2\pi T_R\Gamma^2} \frac{\Omega^2\tau}{e^{\frac{\Omega^2\tau}{2\Gamma}} - 1}, \quad (4)$$

which indicates that the shift is proportional to the initial population difference $\Delta\rho_0$ between the clock states. This dependence is potentially quite useful because we can easily operate the clock by intertwining different preparations by operating with or without the repump laser at the end of the cooling stage so that the shift is modulated and the clock mean frequency is essentially unaffected.

3) *Doppler-related effects:* As the cold atom cloud is interrogated by a traveling wave during free fall, it is sensitive to gravity and any residual velocity or acceleration. If the CPT beams are set to propagate along gravity, the relative frequency shift can be as high as 3×10^{-10} for $T_R = 10$ ms. If the beams are set perpendicular to gravity, a one degree angular deviation produces a shift of 6×10^{-12} . We will study whether or not a standing wave interrogation or an *ab initio* compensation of the Doppler shift is metrologically feasible.

ACKNOWLEDGMENT

The authors thank Terry Brown and James Fung-A-Fat from JILA's Electronic Shop for developing the PLL circuit. F-X Esnault is grateful to the Delegation Generale pour l'Armement and NIST for providing the post-doc fellowship. This paper is a contribution of the National Institute of Standards and Technology, an agency of the U.S. government, and is not subject to copyright.

REFERENCES

- [1] J. Vanier, "Atomic clocks based on coherent population trapping: a review," *Appl. Phys. B*, vol. 81, no. 4, pp. 421–442, 2005.
- [2] S. Knappe, "Emerging topics : MEMS atomic clocks," *Comp. Microsys.*, vol. 3, pp. 571–612, 2007.
- [3] R. Lutwak, "The Chip-Scale atomic clock - recent developments," in *Proc. 2009 Joint Meeting IEEE Int. Frequency Control Symp. and EFTF Conf.*, Besancon, France, 2009, pp. 573–577.
- [4] E. Arimondo, "Coherent population trapping in laser spectroscopy," in *Progress in Optics. Elsevier Science Publication B V, Amsterdam, The Netherlands*, vol. 35, 1996.
- [5] A. V. Taichenachev, V. I. Yudin, V. L. Velichansky, and S. A. Zibrov, "On the unique possibility of significantly increasing the contrast of dark resonances on the D1 line of 87 Rb," *JETP Lett.*, vol. 82, no. 7, pp. 398–403, 2005.
- [6] E. Breschi, G. Milet, G. Kazakov, B. Matisov, R. Lammegger, and L. Windholz, "Study of the laser linewidth influence on "lin || lin" coherent population trapping," in *Proc. 2007 Joint Meeting IEEE Int. Frequency Control Symp. and EFTF Conf.*, 2007, pp. 617–622.
- [7] E. Breschi, G. Kazakov, R. Lammegger, G. Milet, B. Matisov, and L. Windholz, "Quantitative study of the destructive quantum-interference effect on coherent population trapping," *Phys. Rev. A*, vol. 79, no. 6, p. 063837, 2009.
- [8] S. A. Zibrov, I. Novikova, D. F. Phillips, R. L. Walsworth, A. S. Zibrov, V. L. Velichansky, A. V. Taichenachev, and V. I. Yudin, "Coherent population trapping resonances with linearly polarized light for all-optical miniature atomic clocks," *0910.4703*, Oct. 2009.
- [9] E. E. Mikhailov, T. Horrom, N. Belcher, and I. Novikova, "Performance of a prototype atomic clock based on lin||lin coherent population trapping resonances in Rb atomic vapor," *0910.5881*, Oct. 2009.
- [10] K. Watabe, T. Ikegami, A. Takamizawa, S. Yanagimachi, S. Ohshima and S. Knappe, "High-contrast dark resonances with linearly polarized light on the D1 line of alkali atoms with large nuclear spin," *App. Opt.* vol. 48, pp. 1098–1103, 2009.
- [11] P. R. Hemmer, S. Ezekiel, and J. C. C. Leiby, "Stabilization of a microwave oscillator using a resonance raman transition in a sodium beam," *Opt. Lett.*, vol. 8, no. 8, pp. 440–442, 1983.
- [12] P. R. Hemmer, G. P. Ontai, and S. Ezekiel, "Precision studies of stimulated-resonance raman interactions in an atomic beam," *J. Optical Soc. Am. B*, vol. 3, no. 2, pp. 219–230, 1986.
- [13] P. R. Hemmer, M. S. Shahriar, V. D. Natoli, and S. Ezekiel, "Ac stark shifts in a two-zone raman interaction," *J. Optical Soc. Am. B*, vol. 6, no. 8, pp. 1519–1528, 1989.
- [14] T. Zanon, S. Guerandel, E. de Clercq, D. Holleville, N. Dimarcq, and A. Clairon, "High contrast ramsey fringes with Coherent-Population-Trapping pulses in a double lambda atomic system," *Phys. Rev. Lett.*, vol. 94, no. 19, 2005.
- [15] G. Pati, K. Salit, R. Tripathi, and M. Shahriar, "Demonstration of Raman-Ramsey fringes using time delayed optical pulses in rubidium vapor," *Opt. Commun.*, vol. 281, no. 18, pp. 4676–4680, 2008.
- [16] D. M. Farkas, K. M. Hudek, E. A. Salim, S. R. Segal, M. B. Squires, and D. Z. Anderson, "A compact, transportable, Microchip-Based system for high repetition rate production of Bose-Einstein condensates," *0912.0553*, Dec. 2009.
- [17] D. M. Farkas, A. Zozulya, and D. Z. Anderson, "A compact Microchip-Based atomic clock based on ultracold trapped Rb atoms," *0912.4231*, Dec. 2009.
- [18] D. G. Enzer and W. M. Klipstein, "Performance of the PARCS testbed cesium fountain frequency standard," in *Proc. 2004 IEEE Int. Frequency Control Symp.*, 2004, pp. 775–780.
- [19] G. Kazakov, B. Matisov, I. Mazets, G. Milet, and J. Delporte, "Pseudoresonance mechanism of all-optical frequency-standard operation," *Phys. Rev. A*, vol. 72, no. 6, p. 063408, 2005.
- [20] R. Boudot, S. Guerandel, E. de Clercq, N. Dimarcq, and A. Clairon, "Current status of a pulsed CPT cs cell clock," *IEEE Trans. Instrum. Meas.*, vol. 58, no. 4, pp. 1217–1222, 2009.
- [21] A. Nagel, S. Brandt, D. Meschede, and R. Wynands, "Light shift of coherent population trapping resonances," *Europhys. Lett.*, vol. 48, pp. 385–389, 1999.
- [22] M. Zhu and L. S. Cutler, "Theoretical and experimental study of light shift in a CPT-based Rb vapor cell frequency standard," *32nd Annual Precise Time and Time Interval (PTTI) Meeting, Reston, VA, USA*, pp. 311–324, 2000.

²The expression of the light shift for different Rabi frequencies is calculated in [13]. Our study has shown that results for non-equal Rabi frequencies (e.g., set by the magic ratio) do not differ significantly.